Environmental Science and Pollution Research (2024) 31:51222–51236
https://doi.org/10.1007/s11356-024-34596-w

RESEARCH ARTICLE

Unraveling the interplay of common groundwater ions in arsenic removal by sulfide-modified nanoscale zerovalent iron

Payel Singh[1,5] · Penumaka Nagababu[2,5] · Manash R. Das[3,5] · Priyanka Mondal[4,5] · Subhamoy Bhowmick[1,5]

Received: 11 January 2024 / Accepted: 29 July 2024 / Published online: 6 August 2024

Abstract

Sulphidation of nZVI (S-nZVI) has shown to significantly improve the arsenic removal capacity of nZVI, concurrently modifying the sequestration mechanism. However, to better apply S-nZVI for groundwater arsenic remediation, the impact of groundwater coexisting ions on the efficacy of arsenic uptake by S-nZVI needs to be investigated. This present study evaluates the potential of S-nZVI to remove arsenic in the presence of typical groundwater coexisting ions such as Cl^-, HA, HCO_3^-, PO_4^{3-} and SO_4^{2-} through batch adsorption experiments. Individually, PO_4^{3-} and HA had a dominant inhibition effect, while SO_4^{2-} promoted As(III) removal by S-nZVI. Conversely, for As(V) removal, HCO_3^- and SO_4^{2-} impeded the removal process. X-ray spectroscopic investigation suggests that the coexisting ions can either compete with arsenic for the adsorption sites, influence the S-nZVI corrosion rates and/or generate distinct corrosion products, thereby interfering with arsenic removal by S-nZVI. To investigate the cumulative effects of these ions, a 2^{5-1} Fractional Factorial Design of experiments was employed, wherein the concentration of all the ions were varied simultaneously in an optimized manner, and their impact on arsenic removal by S-nZVI was observed. Our results shows that when these ions are present concurrently, PO_4^{3-}, SO_4^{2-} and HA still exerted a dominant influence on As(III) removal, whereas HCO_3^- was the main ions affecting As(V) removal, although the combined influence of the ions was not merely a summation of their individual effects. Overall, the finding of our study might provide valuable insight for predicting the actual performance of S-nZVI in field-scale applications for the remediation of arsenic-contaminated groundwater.

Keywords Adsorption · Arsenic · Coexisting ions · Fractional Factorial Design · S-nZVI

Introduction

Arsenic contamination of groundwater across different geographical regions presents a serious threat to public and environmental health (Bhowmick et al. 2013; Podgorski and Berg 2020). Arsenic exposure from contaminated groundwater-sourced drinking water can result in diverse health complications including cancers of various organs (Khan et al. 2020; Palma-Lara et al. 2020). Arsenic dissolved in groundwater are primarily present as arsenite (As(III)) and arsenate (As(V)) oxyanions in different proportions depending upon the pH and redox potential of the aquifer (Sharma and Sohn 2009; IARC 2012; Bhowmick et al. 2013). The toxicity of these arsenic species are also different and it is generally regarded that As(III) are more toxic than the As(V) species (Sharma and Sohn 2009; IARC 2012). Cleanup of arsenic-contaminated groundwater presents a challenging task and, therefore, new and improved methods are being continuously researched to eliminate arsenic from groundwater.

Responsible Editor: Guilherme Luiz Dotto

✉ Subhamoy Bhowmick
subhamoy081984@gmail.com;
subhamoy.bhowmick@hotmail.com

[1] Kolkata Zonal Center, CSIR-National Environmental Engineering Research Institute (NEERI), Kolkata, West Bengal 700107, India

[2] Environmental Materials Division, CSIR-National Environmental Engineering Research Institute (NEERI), Nehru Marg, Nagpur 440 020, India

[3] Advanced Materials Group, Materials Sciences and Technology Division, CSIR-North East Institute of Science and Technology, Jorhat 785006, India

[4] Membrane and Separation Technology Division, CSIR-Central Glass and Ceramic Research Institute, 196, Raja S.C. Mullick Road, Kolkata 700 032, India

[5] Academy of Scientific and Innovative Research (AcSIR), Ghaziabad 201002, India

Nanoscale zerovalent iron (nZVI) has received the attention of the scientific community due to its high reactivity towards a range of organic and inorganic contaminants (Zou et al. 2016; Li et al. 2017; Liu et al. 2018). Arsenic also has high affinity toward nZVI and is effectively removed from aqueous solution (Ling and Zhang 2017; Wu et al. 2017). However, nZVI tends to rapidly aggregate and surface passivate, resulting in reduced reactivity and mobility, particularly in in situ remediation (Guan et al. 2015). The inherent corrosion reaction of Fe^0 with water results in formation of surface iron oxide/hydroxide layer, which reduces the nZVI reactive lifetime (Liu et al. 2017; Deng et al. 2023). Numerous efforts are being researched to increase nZVI reactivity, which includes stabilizing nZVI particles with stabilizer (Zhao et al. 2016; Mondal et al. 2018), doping noble metal on nZVI (O'Carroll et al. 2013; Wang et al. 2019) and loading nZVI onto some support (Bhowmick et al. 2014; Zou et al. 2016; Wang et al. 2017). Most recently, there have been studies which have documented increased reactivity of nZVI for both organic and inorganic contaminants when modified with lower valent sulfur compounds (Rajajayavel and Ghoshal 2015; Dong et al. 2018; Garcia et al. 2021; Li et al. 2021a). Such sulfidated nZVI (S-nZVI) also reduces the background corrosion reaction with water and increases the reactive lifetime, as well as improves the particle reactivity and selectivity (Gu et al. 2019; Xu et al. 2021). Reports suggest that the reactivity of S-nZVI is strongly dependent upon the S/Fe molar ratio (Rajajayavel and Ghoshal 2015; Dong et al. 2018), although limited but recent investigations suggest that there is clear improvement of arsenic removal efficiency for S-nZVI compared to nZVI (Singh et al. 2021; Zhao et al. 2021). In fact, sulfide modification of nZVI also changed the arsenic sequestration mechanism in comparison to bare nZVI (Singh et al. 2021; Zhao et al. 2021). In the case of nZVI, arsenic is primarily removed by forming Fe–As (co)precipitate and adsorption as surface complex onto nZVI (Yan et al. 2012; Ling and Zhang 2017; Wu et al. 2017). However, for S-nZVI, along with (co)precipitation and adsorption, arsenic is also removed by surface precipitation as iron–sulfide complex (Singh et al. 2021; Zhao et al. 2021).

Notably, for successful field-scale application and deployment of S-nZVI for arsenic removal from contaminated groundwater, it is important to evaluate the impact of co-occurring ions since arsenic adsorption onto an adsorbent is known to be influenced by the presence of several cations and anions (Su and Puls 2001; Mak et al. 2009; Frau et al. 2010; Sun et al. 2016). There are different types of ions that are present in groundwater and these co-occurring ions can compete with arsenic for the surface adsorption sites on the adsorbent and can also alter the electrostatic charge of the adsorbent surface, thereby influencing the overall arsenic removal capacity (Pincus et al. 2020; Zubair et al. 2022). Since the concentrations of the coexisting ions in groundwater are in much higher concentration compared to arsenic, such effects cannot be neglected.

One-factor-at-a-time experimental design is a conventional design to study the effect of such coexisting ions where the response is tested against one factor while keeping the other factors constant. However, such approach has limitations as large number of experimental runs are required which are time-consuming and utilize lots of resources. Moreover, the results of such experimental design are inconclusive as the effects of interactions between parameters are not accounted. To circumvent such shortcoming, statistical design of experiment is being increasingly applied to optimize the interaction between parameters with reasonably reduced number of experiments (Liu et al. 2016; Watson et al. 2016; Li et al. 2021b). For this purpose, Fractional Factorial Design (FFD) is commonly applied. FFD employs orthogonal experimental design where the significant factors as well as interactions between factors are identified without neglecting the interactions of other factors (Montgomery 2001; Box et al. 2005). Tanboonchuy et al. (2012) used FFD to study the competitive behavior of multi-ion on arsenic adsorption onto nZVI and reported inhibiting effect of phosphate (PO_4^{3-}) and humic acid (HA) while enhancing effect of calcium (Ca^{2+}). However, to the best of our knowledge, there has been no report on the effect of coexisting species on arsenic removal by S-nZVI.

The primary aim of the present study was to study the effect of five commonly occurring groundwater ions (Cl^-, HA, HCO_3^-, PO_4^{3-}, SO_4^{2-}) on the arsenic removal efficiency using S-nZVI as adsorbent. The anions were chosen based on their abundance in arsenic-contaminated groundwater and their relationship with arsenic mobilization (Bhowmick et al. 2013; Malik et al. 2020). The individual and combined effect of coexisting ions was screened, and optimization of adsorption efficiency was performed using FFD. The results obtained from this study will therefore help to increase our understanding on the potential feasibility of S-nZVI for in situ remediation of arsenic-contaminated groundwater in the presence of co-occurring background species.

Materials and methods

Chemicals and reagents

All the chemicals were used without any prior treatment. To synthesize the S-nZVI, $FeCl_3$ (≥ 98%), $NaBH_4$ (96%) and $Na_2S_2O_4$ (85%) were purchased from Merck, Spectrochem and Loba Chemie respectively. For batch experiment, stock solutions of coexisting ions were prepared using NaH_2PO_4 (99.5%, Sigma-Aldrich), Na_2SO_4 (≥ 99%, Sigma-Aldrich), NaCl (99.9%, Avantor), $NaHCO_3$ (99.5%,

Sigma-Aldrich) and humic acid (Sigma-Aldrich) for PO_4^{3-}, SO_4^{2-}, Cl^-, HCO_3^- and HA respectively. $NaAsO_2$ (98%) and $NaHAsO_4{\cdot}7H_2O$ (98%) were brought from Nice chemicals and were used to prepare As(III) and As(V) stock solutions respectively. HCl (37%) and NaOH (≥97%) were supplied by Merck. All the solutions were prepared using Milli-Q water.

Synthesis methods of S-nZVI

S-nZVI was prepared according to one-step route and the details are given in the Supplementary Information (Text S1). The S/Fe molar ratio of the synthesized S-nZVI was selected as 0.1 for all the experiments based on the maximum reactivity of S-nZVI for As(III) and As(V) at that particular S/Fe ratio obtained in our previous study (Singh et al. 2021).

Batch adsorption experiments

All the batch experiments for arsenic uptake by S-nZVI were done under anaerobic condition. The adsorption experiments were performed in 50-mL centrifuge tube containing 5 mg/L of either As(III) and As(V) solution, 0.05 g/L S-nZVI and appropriate amount of background species. The initial pH was adjusted to 7.00 ± 0.05 with NaOH and HCl and the centrifuge tube was placed in rotating shaker at 30 rpm. Periodically, sample aliquot (5 mL) was withdrawn from the centrifuge tube and filtered through 0.22-µm syringe filter (Moxcare). The filtered samples were measured for arsenic and iron in ICP–OES (Prodigy high dispersion ICP, Teledyne–Leeman Labs). All the experiments and analysis were carried out in triplicates to avoid occasional results. To investigate the surface morphology, the formation of various iron phases and the change in elemental valence state composition after reaction, transmission electron microscopy (TEM), X-ray diffraction (XRD) and X-ray photoelectron spectroscopy (XPS) analysis were performed on the reacted S-nZVI. The reacted S-nZVI was collected after the end of reaction, washed with deoxygenated Milli-Q water and dried in vacuum oven. The dried reacted S-nZVI samples were later analyzed for TEM (Technai G2 30ST-FEI, USA), XRD (1710 diffractometer, Philips, Netherlands) and XPS (ESCALAB Xi + spectrometer, Thermo-Scientific).

Assessment of single species effect

The effect of individual co-occurring species was evaluated by spiking separate amounts of coexisting ions in centrifuge tube along with arsenic solution and S-nZVI. The concentration for each of the coexisting ions were as follows: PO_4^{3-}, 2 and 10 mg/L; SO_4^{2-}, 5 and 50 mg/L; HCO_3^-, 50 and 500 mg/L; Cl^-, 10 and 200 mg/L; HA, 1 and 10 mg/L. All solutions that were prepared for each of the anions were stable, as the concentrations were well below the solubility limit of the respective salts (Table S1).

Assessment of multi-species effect

In this work, the five co-occurring background ions (factors) namely, Cl^-, HA, HCO_3^-, PO_4^{3-} and SO_4^{2-} were screened for their effect on arsenic removal percentage (response) by S-nZVI. Design of experiment (DOE) approach was employed to classify the major effects and provide insights about the changes of response that happen due to deviation in factor levels (Montgomery 2001; Antony 2003; Box et al. 2005). The adsorption experiments were performed in consonance with the 2^{k-p} FFD, where k denotes the number of factors (which was 5 in this study), and p represents the degree of fractionation (degree of fractionation was 1 in this case). By adopting two-level FFD and using two different concentration levels (the lower concentration was noted by minus (−) sign and the higher concentration was presented by plus (+) sign) for all the five factors, it was possible to decrease the total number of experimental runs to 16 instead of 32 for full factorial design (Table 1). The high and low concentration for each of the factors was selected based on the single species system. The applied IV resolution was particularly useful as it covered estimation of all main effects and other two-factor interactions except three-factor and other higher factor interactions which were confounded with main effect contributors (Montgomery 2001). It was

Table 1 Experimental design matrix for 2^{5-1} FFD with resolution IV

Run number	Factors and codes				
	HCO_3^-	Cl^-	HA	PO_4^{3-}	SO_4^{2-}
	A	B	C	D	E = ABCD
1	−1	−1	−1	−1	1
2	1	−1	−1	−1	−1
3	−1	1	−1	−1	−1
4	1	1	−1	−1	1
5	−1	−1	1	−1	−1
6	1	−1	1	−1	1
7	−1	1	1	−1	1
8	1	1	1	-1	−1
9	−1	−1	−1	1	−1
10	1	−1	−1	1	1
11	−1	1	−1	1	1
12	1	1	−1	1	−1
13	−1	−1	1	1	1
14	1	−1	1	1	−1
15	−1	1	1	1	−1
16	1	1	1	1	1

found that the variable E as generator confounded as follows: E = A × B × C × D (Table 1). All the analysis was performed using the Minitab software.

Results and discussion

Selection of experimental parameters

In our previous study, Singh et al. (2021) synthesized S-nZVI using a one-step approach with sodium dithionite as the sulfidating agent. It was found that the S/Fe molar ratio of S-nZVI strongly influenced its arsenic removal performance, with an S/Fe ratio of 0.1 showing the highest removal efficiency for both As(III) and As(V). Additionally, the incorporation of sulfur onto the nZVI particle partially mitigated the aging effect and the reduced reactivity of the nZVI particle over time, a major limitation for the nZVI particles. Our investigation into the arsenic sequestration mechanism revealed that sulfur modification of nZVI altered the arsenic removal process. For nZVI, As(III) and As(V) were primarily removed through co-precipitation, adsorption and reduction, with nZVI capable of reducing As(III) and As(V) to its lower valence states, including As(0). In contrast, reduction of As(III) and As(V) species was not observed for S-nZVI, instead the uptake of As(III) oxyanion by S-nZVI was through adsorption onto the surface of S-nZVI along with As_2S_3-like surface precipitate (Singh et al. 2021). Therefore, our previous study successfully demonstrated the potentiality of S-nZVI and optimized the S/Fe ratio for enhanced removal of As(III) and As(V), and also elucidated the change in As removal mechanism from such sulfur modification in nZVI. However, for practical application and effective field-scale deployment of S-nZVI, it is crucial to understand how groundwater contaminants might impact arsenic removal by competing for the adsorption sites and affecting iron corrosion (Frau et al. 2010; Mangayayam et al. 2020; Pincus et al. 2020; Zubair et al. 2022). This present study focuses on examining these influences in detail and investigating how co-existing groundwater ions might affect the arsenic removal process using S-nZVI.

In this present investigation, we employed batch adsorption reaction condition. In this context, the rate of mixing is an important parameter as it might significantly affect the mass transport and iron dissolution (Polasek 2007; Epolito et al. 2008; Noubactep et al. 2009; Sun et al. 2016). Earlier report suggests that mass transport influences the contaminant removal for ZVI-based adsorbent surfaces, where a relationship exists between the reaction rate and the speed of mixing (Agarwal and Tratnyek 1995). Generally, the formation of an oxide shell on ZVI particles impedes the mass transport of contaminants to the adsorbent. While disrupting the oxide shell formation might seem advantageous, this shell plays a crucial role in contaminant removal (Yan et al. 2010; Mu et al. 2017; Di et al. 2023). Increasing the proximity of the contaminant species to the iron surface and enhancing the dissolution of the solid phase can improve the material performance (Noubactep et al. 2009). Mixing achieves this by reducing nZVI aggregation, exposing fresh Fe^0 and removing corrosion products from the solution (Noubactep et al. 2009).

It is important to note that the mechanism of Fe corrosion and the characteristics of the corrosion products differ under aerobic and anaerobic conditions (Filip et al. 2014; Liu et al. 2017; Deng et al. 2023; Mundra et al. 2023). In the literature, there has been a wide range of mixing speed that has been used for removal of contaminants by Fe-based adsorbent (especially nZVI), with some studies employing speeds up to 250 rpm and more under anoxic conditions (Yan et al. 2012; Lv et al. 2019; Liang et al. 2019; Liang et al. 2021). However, conventional studies have typically applied mixing speed below 50 rpm (Matheson and Tratnyek 1994; Agarwal and Tratnyek 1995). For instance, Kim et al. (2011) applied 15-rpm mixing speed to study the degradation of TCE by FeS/Fe^0 system. Similarly, mixing speeds of 30–40 rpm have been used for the removal of heavy metals and organic contaminants by S-nZVI (Gong et al. 2017; Xu et al. 2019). In this context, Noubactep et al. (2009) investigating the effect of shaking intensity on discoloration of methylene blue by metallic iron concluded that shaking intensities intended to promote contaminant mass transfer to the Fe surface should be limited to a maximum of 50 rpm. The study further recommended that experiments relevant to subsurface Fe/H_2O systems should be conducted under shaking conditions that simulate the velocities characteristic of groundwater flow. In another study, Epolito et al. (2008) suggested that the type of mixing, such as end-over-end rotation or orbital shaking, has more significant impact on the reaction rate rather than the mixing intensity. Therefore, considering the subsurface conditions with low oxygen availability, in this present study, we applied an end-over-end rotation with speed of 30 rpm to ensure minimal disturbance to oxide shell formation while maintaining adequate mass transfer, consistent with the low flow rates in groundwater environments.

Another crucial parameter for this study is the selection of the type and concentration of co-existing ions commonly found in arsenic-contaminated groundwater. Studies focussing on groundwater arsenic have usually reported HCO_3^-, Cl^-, PO_4^{3-} and SO_4^{2-} to be the most dominant ions with some of these ions having an intricate relationship with the arsenic mobilization processes (Nath et al. 2008; Biswas et al. 2011; Bhowmick et al. 2013; Malik et al. 2020). Table S2 provides a brief overview of the variation in these ion concentration in arsenic-contaminated groundwater, as reported in the literature across different aquifers. For instance, in one such study in the Bengal Delta Plain, a

well-known high arsenic groundwater contaminated region, Bhowmick et al. (2013) reported the concentration of PO_4^{3-}, HCO_3^-, Cl^- and SO_4^{2-} in the range of 0.11–4.5, 168–515, 65–426 and 2.9–52 mg/L respectively. Similarly, in Santiago del Estero Province, Argentina, large spatial variability of these ion concentrations has been reported. Bhattacharya et al. (2006) found 208–1998 mg L^{-1} HCO_3^-, 62.6–1434 mg L^{-1} Cl^-, 84–4826 mg L^{-1} SO_4^{2-} and 0.02–4.80 mg L^{-1} PO_4^{3-} in the collected groundwater samples from Río Dulce alluvial cone. Similarly, Bundschuh et al. (2004) reported HCO_3^- concentrations of 12–1893 mg/L, Cl^- of 1.3–2716 mg/L and SO_4^{2-} of 19–1368 mg/L in samples from the Chaco-Pampean Plain. Therefore, in this present study, we considered a generalized range for these four ions so as to cover both the higher and lower range: HCO_3^- (50 and 500 mg L^{-1}), Cl^- (10 and 200 mg L^{-1}), PO_4^{3-} (2 and 10 mg L^{-1}) and SO_4^{2-} (5 and 50 mg L^{-1}). pH of the solution was adjusted to 7.00 since arsenic-contaminated groundwater generally has a circum-neutral pH (Table S2). Additionally, 1 and 10 mg L^{-1} of HA were used to study the effect of dissolved organic matter, based on the concentration reported in the literature (Mak et al. 2009; Liu et al. 2013; Malik et al. 2020).

Once the experimental parameters were optimized, in the following section, we specifically try to understand the mode of influence of the selected coexisting ions on the arsenic removal performance of S-nZVI.

Individual effect of ions on arsenic removal by S-nZVI

Phosphate (PO_4^{3-})

It has been widely documented that PO_4^{3-} has an inhibitory effect on arsenic removal due to competitive sorption, as both arsenic and PO_4^{3-} forms inner sphere complex on iron oxide (Frau et al. 2010; Bhowmick et al. 2014; Sun et al. 2016). In this present study, we found that the decrease in arsenic adsorption on S-nZVI was much more pronounced for As(III) compared to As(V) in the presence of PO_4^{3-} (Fig. 1a). For example, the percentage As(III) removal decreased from 90.50% (in absence of PO_4^{3-}; $t = 2$ h) to 77.11% (2 mg/L PO_4^{3-}; $t = 2$ h) and down to 58.76% at

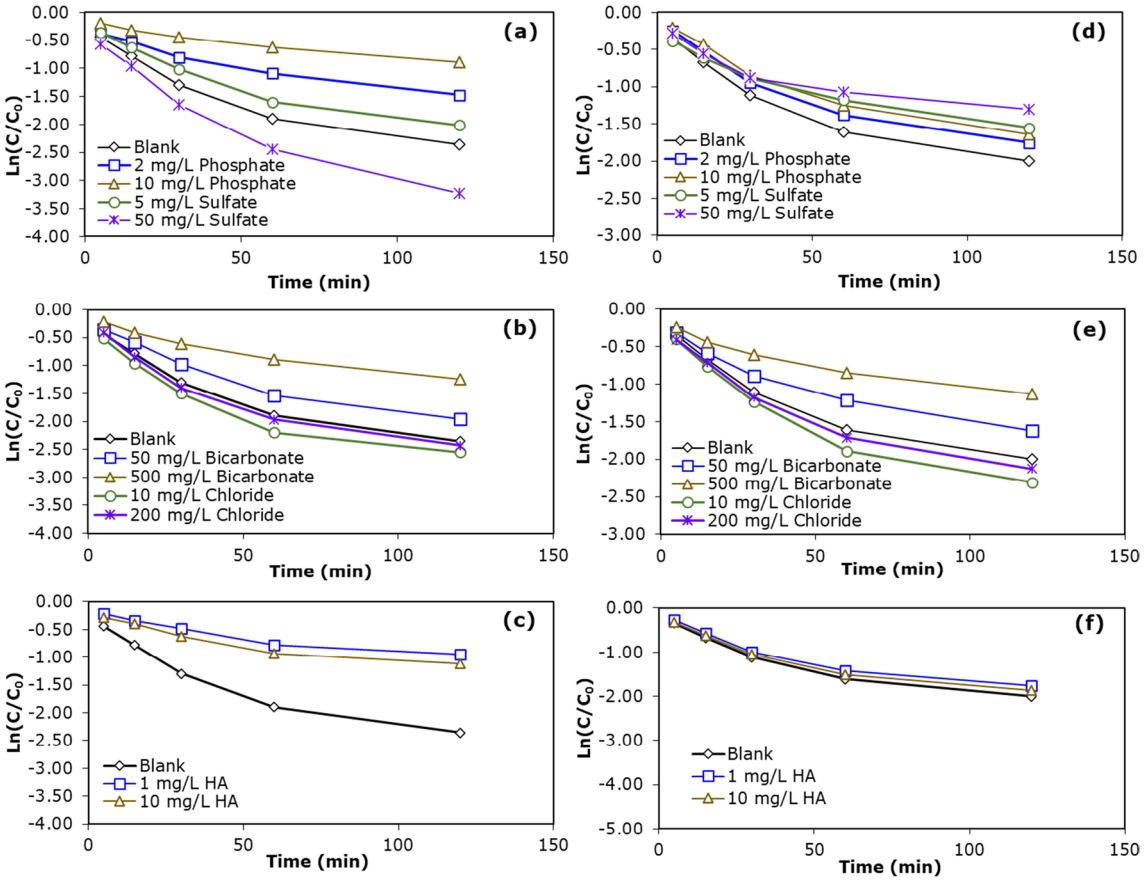

Fig. 1 Effect of PO_4^{3-}, SO_4^{2-}, HCO_3^-, $Cl.^-$ and HA on As(III) (**a**, **b**, **c**) and As(V) (**d**, **e**, **f**) removal by S-nZVI. Experimental condition: [S-nZVI]: 0.05 gm/L; initial [As (III)]: 5 mg/L; pH: 7.0 ± 0.05

10 mg/L PO_4^{3-} solution ($t = 2$ h) (Fig. 1a). In the case of As(V), the percentage As(V) removal decreased from 86.49 to 82.66% and 80.59% in blank, 2 mg/L and 10 mg/L of PO_4^{3-} solution, respectively ($t = 2$ h) (Fig. 1d).

Fig. S1 shows the TEM images of the S-nZVI after reaction with As(III) and As(V) in the presence of PO_4^{3-}. Both the particles exhibit a core shelled structure with a well-formed outer oxide layer, suggesting oxidation of the S-nZVI particles after reaction. To investigate further, XPS analysis of the reacted S-nZVI was performed. It was found that with increase in PO_4^{3-} concentration, there is an increase in relative percentage of Fe(II) and S^{2-} peaks, for both As(III) and As(V) (Figs. 2 and 3; Table S3). The increase in peaks of Fe(II) and S^{2-} indicates presence of more surface FeS on the reacted S-nZVI and, therefore, signifies decrease in corrosion of S-nZVI with increase in PO_4^{3-} concentration. Such decrease in S-nZVI corrosion affects the As–Fe co-precipitation as evidenced from the increase in solution

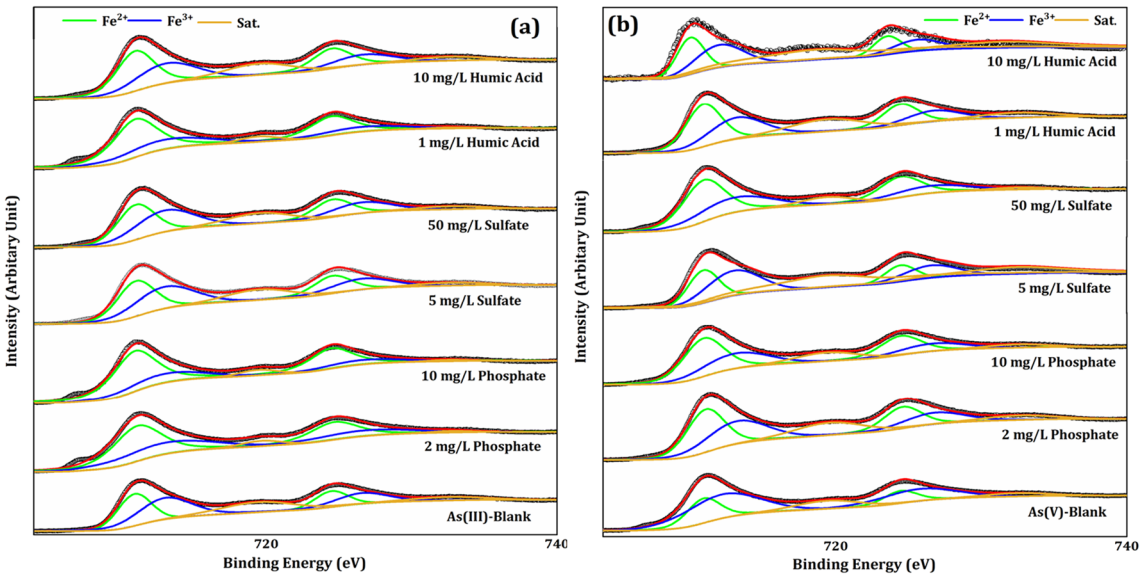

Fig. 2 Fe2p spectrum of **a** As(III)- and **b** As(V)-reacted S-nZVI in the presence of PO_4^{3-}, SO_4^{2-} and HA. Experimental condition: [S-nZVI]: 2 gm/L; initial [As]: 100 mg/L; pH: 7.0 ± 0.05

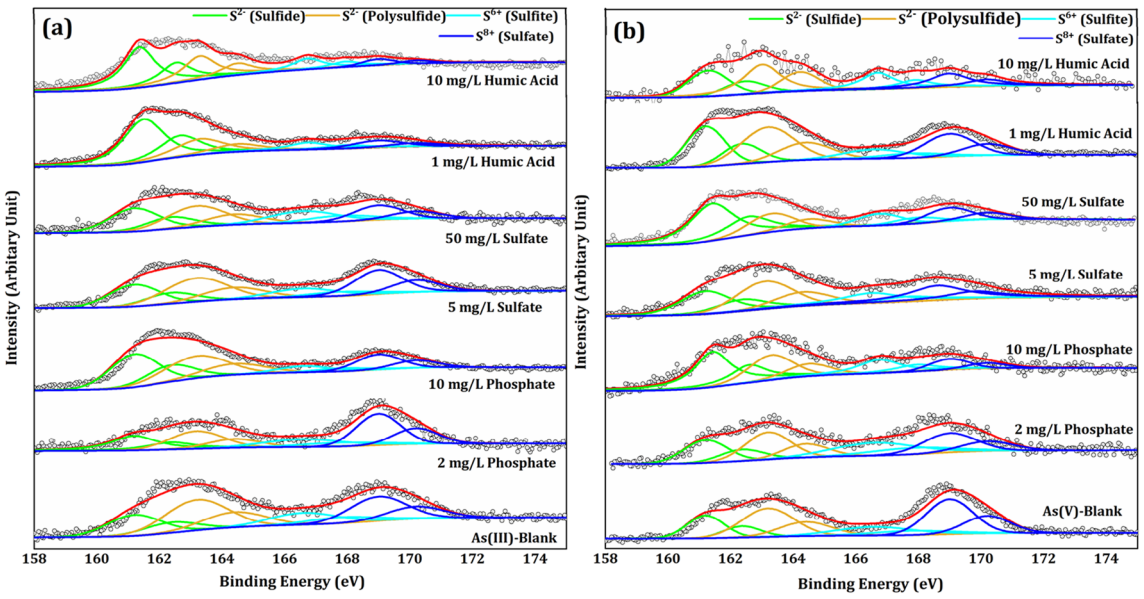

Fig. 3 S2p spectrum of **a** As(III)- and **b** As(V)-reacted S-nZVI in the presence of PO_4^{3-}, SO_4^{2-} and HA. Experimental condition: [S-nZVI]: 2 gm/L; initial [As]: 100 mg/L; pH: 7.0 ± 0.05

Fe concentration with increase in PO_4^{3-} concentration (Fig. S2), which eventually leads to the decrease in As removal. Additionally, As3d spectrum for As(III)-reacted S-nZVI shows that there is also a substantial decrease in As_2S_3 peaks when the PO_4^{3-} concentration increases from blank solution to 2 to 10 mg/L (Fig. 4a; Table S3). Since PO_4^{3-} competes with As(III) for the adsorption sites on the S-nZVI, there is eventually a decrease in interaction of adsorbed As(III) and surface FeS and, thereby, resulting in a decrease in As_2S_3 surface precipitate formation and As(III) removal (Fig. 1a). However, in the case of As(V), with increase in PO_4^{3-} concentration, there is less substantial change in surface speciation of arsenic, including As_2S_3 peaks (Fig. 4b; Table S3). Given that As(V) is largely removed by outer sphere complexation by S-nZVI and only a small amount of As_2S_3 precipitate is formed (Singh et al. 2021), there is less significant decrease in As(V) adsorption capacity in the presence of PO_4^{3-}. Similar non-significant effect of PO_4^{3-} have also been reported for As(V) removal by FeS (Niazi and Burton 2016; Han et al. 2020).

Sulfate (SO_4^{2-})

In this present investigation, SO_4^{2-} in solution had a negative impact on the removal of As(V) by S-nZVI (Fig. 1d). With increase in SO_4^{2-} concentration from blank to 5 to 50 mg/L, the As(V) removal percentage was 86.49%, 78.90% and 72.73%, respectively. On the contrary, there was a slight decrease in As(III) removal at lower SO_4^{2-} concentration, but the As(III) removal increased significantly when SO_4^{2-} concentration increased from 5 to 50 mg/L (Fig. 1a). Such incremental increase in As(III) removal at higher SO_4^{2-} concentration was concurrent with simultaneous decrease in dissolved Fe (Fig. S2).

There has been a previous report which suggested a minor decrease in arsenic removal in the presence of SO_4^{2-} due to electrical repulsion between negatively charged SO_4^{2-} and arsenic species (Sun et al. 2006), and/or decrease in adsorption sites from replacement of surface iron (oxy)hydroxides with SO_4^{2-} (Tanboonchuy et al. 2012; Zubair et al. 2022). Microscopic images of the reacted S-nZVI in the presence of SO_4^{2-} reveal that for As(V), the core of the particles remains more intact, as indicated by the darker spots, and the outer oxide shell is better developed, suggesting passivation of the S-nZVI particles (Fig. S1). Conversely, for As(III)-reacted S-nZVI, the outer layer appears more diffused and the inner core of the particles is significantly lighter, indicating increased corrosion of the particles.

XPS analysis of the As(V)—reacted samples showed that at low SO_4^{2-} concentration, the peaks of both Fe(II) and S^{2-} did not change considerably when compared to blank As(V)—reacted samples (without the presence of background ions) (Figs. 2 and 3). However, when the SO_4^{2-} concentration was increased to 50 mg/L, there was an increase in peaks of Fe(II) and S^{2-} in the samples after reaction with As(V), indicating decrease in S-nZVI corrosion, in agreement with the TEM image (Figs. 2b and 3b). Additionally, the As3d spectrum showed that there was no significant change in percentage of As_2S_3 peaks on the surface of As(V)—reacted S-nZVI with change in SO_4^{2-} concentration (Fig. 4b; Table S3). Consequently, based on the above results, it can be inferred that the adverse impact of

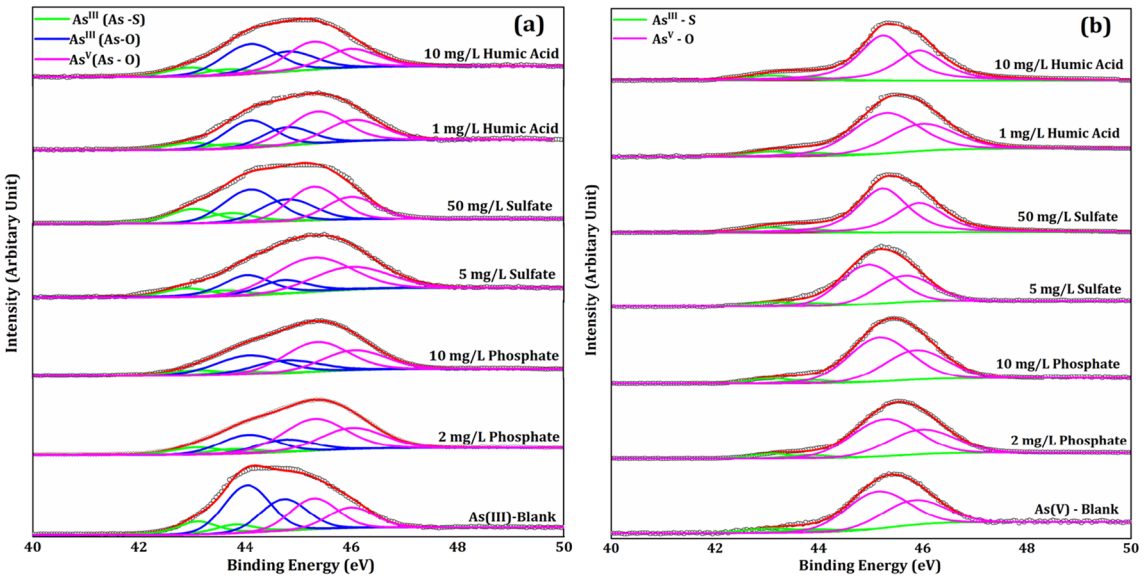

Fig. 4 As3d spectrum of **a** As(III)- and **b** As(V)-reacted S-nZVI in the presence of PO_4^{3-}, SO_4^{2-} and HA. Experimental condition: [S-nZVI]: 2 gm/L; initial [As]: 100 mg/L; pH: 7.0 ± 0.05

SO_4^{2-} on As(V) removal was due to reduction in the corrosion of S-nZVI corrosion and the inhibition in As(V) complex formation.

On the other hand, Fe2p spectrum of As(III)-reacted S-nZVI samples showed a shift towards the lower binding energy when the SO_4^{2-} concentration was increased, suggesting presence of more Fe^{2+} species on the surface of reacted S-nZVI (Fig. 2a). However, the S2p spectrum showed that there was no substantial increase in the peaks of S^{2-} when the SO_4^{2-} concentration was increased and the peak area of S^{2-} remained nearly constant (Fig. 3a). Furthermore, it was found that at lower SO_4^{2-} concentration, there was a slight decrease in the As_2S_3 peaks, but the As_2S_3 peak area increased considerably at higher SO_4^{2-} concentration, as evidenced from the As3d spectrum (Fig. 4a; Table S3). Thus, from the results of the XPS analysis, it may be concluded that at lower SO_4^{2-} concentration, the decrease in As(III) removal was due to reduced S-nZVI corrosion, whereas the increase in As(III) removal in the presence of high SO_4^{2-} concentration might be attributed to excess surface precipitation of arsenic sulfide and iron sulfides, thereby also accounting for the observed reduction of dissolved Fe (Fig. S2). Notably, in reduced sulfidic environment, formation of FeS and As_2S_3 precipitation is promoted, as reported in recent studies (Shakya and Ghosh 2018; Shakya et al. 2019).

Bicarbonate (HCO_3^-)

As shown in Fig. 1, the presence of low concentration of HCO_3^- marginally retarded the removal of As(III), but for As(V), the arsenic removal performance was significantly inhibited. However, when the HCO_3^- concentration increases from 50 to 500 mg/L, there was a sharp decrease in arsenic removal efficiencies for both As(III) and As(V) (from 85.78 to 71.28%, and 80.20 to 67.88% for As(III) and As(V), respectively) (Fig. 1b, e). Since HCO_3^- can also form inner sphere surface complex with iron oxide (Yang et al. 2015; Zubair et al. 2022), it is expected that competition for adsorption sites between arsenic species and HCO_3^- may result in decrease in arsenic removal. However, the less inhibition effect of As(III) removal at low HCO_3^- concentration points towards the effectiveness of FeS coating in S-nZVI to mitigate the inhibitive effect of HCO_3^-. It should be noted that in the experimental pH range (7.2–8.9), As(III) usually exists as neutral H_3AsO_3 species, while As(V) as $H_2AsO_4^{2-}$ species (Sharma and Sohn 2009). Thus, uptake of HCO_3^- induces more electrostatic repulsion between the S-nZVI surface and doubly negative charged As(V) oxyanions, resulting in more pronounced decrease in As(V) removal (Fig. 1e). Moreover, there have been reports which suggest that presence of HCO_3^- in higher concentration preferentially leads to formation of chukanovite, carbonate green rust, siderite, etc. mineral-like phases that form a passive layer on the surface (Bi et al. 2009; Mangayayam et al. 2020). XRD analysis of the reacted samples showed that at low HCO_3^- concentration, for both As(III) and As(V), there is presence of magnetite/maghemite as the only corrosion products (Fig. 5). However, at higher HCO_3^- concentration (500 mg/L), small peak of siderite was detected along with magnetite/maghemite (Fig. 5). This suggests that at higher HCO_3^- concentration, iron carbonate mineral is also formed along with iron oxide/hydroxide corrosion products. Such additional precipitation of iron carbonate mineral on the surface of S-nZVI also inhibits the access of arsenic to iron oxide and FeS, thereby impeding arsenic adsorption and co-precipitation reaction for arsenic removal. Figure S1 presents the TEM images of the arsenic-reacted S-nZVI in the presence of HCO_3^-. The well-formed outer layer in the reacted S-nZVI observed in the TEM images points towards the formation of iron oxide and/or iron carbonate minerals

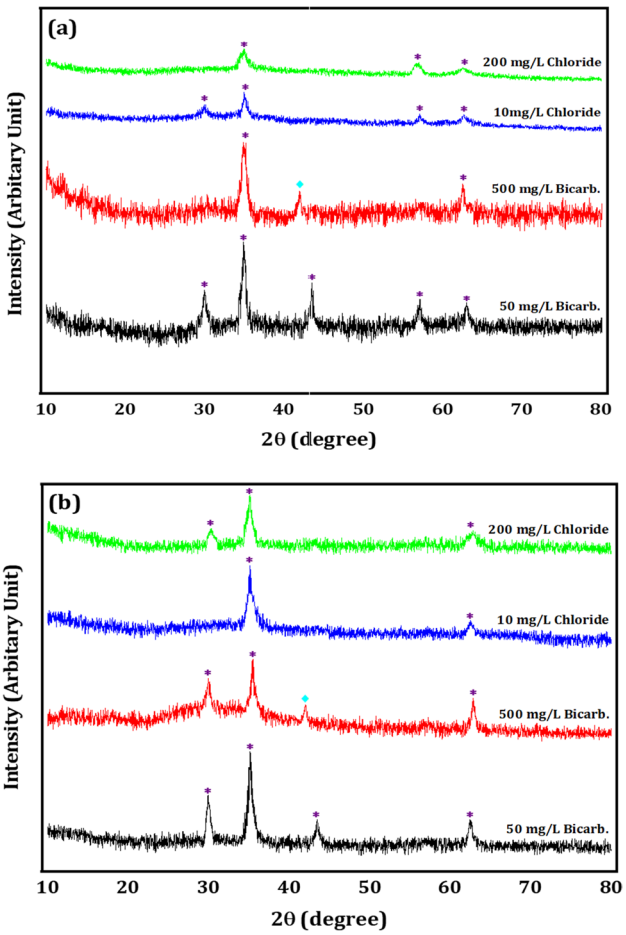

Fig. 5 XRD analysis of **a** As(III)- and **b** As(V)-reacted S-nZVI in the presence of high and low concentration of HCO_3^- and $Cl.^-$. Experimental condition: [S-nZVI]: 2 gm/L; initial [As]: 100 mg/L; pH: 7.0 ± 0.05. (* = magnetite/maghemite; ◇ = siderite)

on the S-nZVI surface, thereby further supporting the findings of the XRD analysis.

Chloride (Cl^-)

The effect of Cl^- on As(III) and As(V) removal is shown in Fig. 1. It was found that at low Cl^- concentration (10 mg/L), there was a slight increase in both As(III) and As(V) removal. However, with further increase in Cl^- concentration from 10 to 200 mg/L, there was a slight decrease in As(III) and As(V) removal (Fig. 1b, e). The observed increase in arsenic adsorption may be due to promotion of iron corrosion (Turcio-Ortega et al. 2012), resulting in increased arsenic adsorption and/or coprecipitation. Also, passive layer formation is inhibited, and new iron oxide layer is produced, since corrosion helps to diffuse the iron oxide layer from the iron surface to the bulk water phase (Rangsivek and Jekel 2005). This is corroborated from the microscopic images which shows that both As(III)- and As(V)-reacted S-nZVI in the presence of Cl^- exhibit a core shelled structure but the outer shell is much distorted and ill-defined (Fig. S1). Moreover, previous studies have shown that Fe-based materials in the presence of high Cl^- concentration leads to precipitation of white rust and chloride green rust (Mangayayam et al. 2020). Such precipitation of iron chloride phases may decrease the number of reactive sites on the S-nZVI surface for arsenic uptake. However, in this study, XRD analysis of the reacted S-nZVI samples did not show any additional peaks of iron chloride minerals apart from iron oxide (magnetite/maghemite) phases even at high chloride concentration (Fig. 5), and may be due to the low concentration of these iron chloride minerals precipitated on the S-nZVI surface.

Humic acid

HA is one of the major components of natural organic matter that is ubiquitously present in aquatic environment. To investigate the effect of HA, As(III) and As(V) adsorption was performed in the presence of low (1 mg/L) and high (10 mg/L) concentration of HA. In low concentration, HA had a substantial inhibitory effect on As(III) removal, while As(V) removal decreased marginally (Fig. 1c, f). On the other hand, when the concentration of HA was increased from 1 mg/L to 10 mg/L, there was a slight increase in arsenic removal for both As(III) and As(V), although the removal percentage was less than the blank solution (Fig. 1c, f). For example, the percentage arsenic removal increased from 61.23 to 67.32% and 82.75 to 84.46% for As(III) and As(V) respectively, when concentration of HA increased from 1 to 10 mg/L.

Fe2p spectrum for both As(III)- and As(V)-reacted S-nZVI shows a slight shift towards lower binding energy at low HA concentration, indicating presence of more Fe(II) species (Fig. 2). Similarly, the S2p spectrum shows relative increase in peaks of S^{2-} for both As(III)- and As(V)-reacted S-nZVI at low HA concentration compared to arsenic-reacted S-nZVI without the presence of HA (Fig. 3). Such observations indicate that the HA might form a protective organic layer on the surface of S-nZVI, thereby inhibiting both iron corrosion and arsenic adsorption (Turcio-Ortega et al. 2012; Fakour et al. 2015). This is consistent with the TEM images of the reacted S-nZVI in the presence of HA where the microstructural feature of the S-nZVI particles shows formation of well-defined outer layer after reaction (Fig. S1). Additionally, at low HA concentration, the As3d spectrum shows significant decrease in As_2S_3 peaks for As(III), but for As(V), there is no substantial change in As_2S_3 peaks (Fig. 4). Thus, it may be further suggested that in the case of As(III), the organic layer additionally blocks the reaction of As(III) with surface FeS of S-nZVI and decreases the surface precipitation of As_2S_3, thereby further retarding the As(III) removal. As for As(V), our results indicate that the extent to which HA forms a coating on the surface of S-nZVI has less influence on the adsorption of As(V) and the observed minimal decrease in As(V) removal could be attributed to reduction in iron corrosion and co-precipitate formation (Fig. 1f).

XPS analysis of As(III)- and As(V)-reacted S-nZVI at high HA concentration shows decrease in peaks of Fe(II) and S^{2-}, suggesting increase in corrosion of S-nZVI (Figs. 2 and 3). On the contrary, As3d spectrum shows there was no considerable change in the surface precipitation of As_2S_3 at high HA compared to low HA, especially for As(III) (Fig. 4; Table S3). Such contrasting results of increased iron corrosion but practically no change in As_2S_3 precipitation might be explained considering the reduced aggregation and enhanced dispersion of S-nZVI particles due to decrease in steric hindrance and electrostatic repulsion between HA adsorbed S-nZVI particles (Du et al. 2020; Yao et al. 2020). In a recent study, Wang et al. (2020) found similar adsorption behavior of Pb^{2+} on polystyrene-supported nano-Fe(0) nanocomposite. The authors concluded that the decrease in Pb^{2+} removal efficiency at low HA concentrations was due to surface-competitive adsorption of Pb^{2+} and HA, whereas at high HA concentration, the Pb^{2+} removal rate remained constant because of increased particles dispersion caused by decrease in electrostatic interactions between the HA-coated nZVI particles.

Evaluation of competitive effects

Effects of different levels of coexisting ions on arsenic removal

To investigate the simultaneous impact of co-existing ion (Cl^-, HA, HCO_3^-, PO_4^{3-}, SO_4^{2-}) on the arsenic removal

capacity of S-nZVI, the concentrations of the ions were systematically varied according to 2^{5-1} FFD (Table 1). Each of the experimental run number corresponds to a solution containing different concentration of the anions mixed together. Figure 6 presents the variation of arsenic removal by S-nZVI with respect to different run number. As discussed previously, due to difference in sequestration mechanism of As(III) and As(V) by S-nZVI and the varying influence of the ions on As(III) and As(V) removal, the profile of As(III) and As(V) removal were differentially affected by the type and concentration of background co-occurring ions (Fig. 6). It can be seen that the highest As(III) removal was observed for run nos. 10 and 15. Both these runs have low concentration of PO_4^{3-} and HA, and high concentration of SO_4^{2-} (Table 1). On the other hand, lowest As(III) removal was observed in run nos. 4 and 16, having high concentration of PO_4^{3-} and HA, and low concentration of SO_4^{2-}. These results suggest that in the presence of all co-existing ions, PO_4^{3-} and HA still exert a dominant inhibitory effect, whereas SO_4^{2-} promotes As(III) removal by S-nZVI.

In the case of As(V), the highest arsenic removal was observed in runs no. 15 and 16; both these runs have low HCO_3^- in solution (Fig. 6). For run nos. 5 and 14, where the concentration of HCO_3^- was set at high levels, the As(V) removal efficiency dropped sharply to 50.2% and 47.8%, respectively (Fig. 6). Therefore, a preliminary conclusion may be drawn that HCO_3^- still has the most significant negative impact on the removal of As(V) by S-nZVI, when all the ions are present together.

Screening of main effects

Analyses of estimate of effect for the investigated factors are shown in Fig. 7. Estimate of effects for a particular factor was tabulated from the difference of that factor's average response at high level variables (+) and low level variables (−) in the design matrix of Table 1 (Tanboonchuy et al. 2012). It can be seen that for As(III), PO_4^{3-} and HA had a negative estimate of effects of − 9.65 and − 7.91, respectively, implying the dominant role of PO_4^{3-} and HA as the main inhibiting factors in As(III) removal in the presence of other co-existing ions (Fig. 7a). For example, when the concentration of PO_4^{3-} increased from 2 to 10 mg/L, the average As(III) removal decreased from 68.71 to 59.06%, and on increasing the concentration of HA from 1 to 10 mg/L, the As(III) removal decreased from 67.84 to 59.93%. On the contrary, SO_4^{2-} had a positive estimates of effects, and the As(III) removal increased by 15.03% when SO_4^{2-} concentration increases from 5 to 50 mg/L (Fig. 7a). The effect of HCO_3^- and Cl^- on As(III) removal was weak in comparison to the other investigated ions when all the ions were present simultaneously. In the case of As(V), HCO_3^- was the main factor that showed negative estimates of effects of − 14.67 (Fig. 7b). This is to say that increasing the concentration of HCO_3^- ions from low to high levels inhibited As(V) removal. Compared to the effect of HCO_3^-, the positive effect of Cl^- and SO_4^{2-} and the negative effect of HA and PO_4^{3-} on As(V) removal were relatively minor (Fig. 7b). These results are in contrast with reports published in the literature on As(V) adsorption on Fe based material, where PO_4^{3-} exhibits the most dominant inhibitory effect, followed by HCO_3^- and SO_4^{2-} (Bhowmick et al. 2014; Frau et al. 2010; Yang et al. 2015; Zubair et al. 2022). This discrepancy underscores the alteration in nZVI particle properties due to sulfur modification, leading to changes in the As(V) adsorption mechanism (Singh et al. 2021). Interestingly, in the multi-ion system, the negative impact of SO_4^{2-} on As(V) removal observed in the single-ion system was not evident; instead, a minor positive effect was found (Fig. 7b). This points towards the complex interplay among coexisting ions during As(V) removal by S-nZVI and the reduction in S-nZVI corrosion due to SO_4^{2-} (as explained earlier) might be compensated by other coexisting ions present in solution.

The above results were confirmed by Pareto chart (Fig. S3) where the vertical line indicates the magnitude of statistically minimum significant effect of 5% significance level, while the factors are represented by horizontal columns and are sequenced based on the decreasing influence for each effect (in this case, arsenic removal) and the length of each of the column being proportional to the degree of significance (Liu et al. 2016). Accordingly, the factors that exceed the vertical line are considered to have a possible significant effect on arsenic removal. It was found that PO_4^{3-},

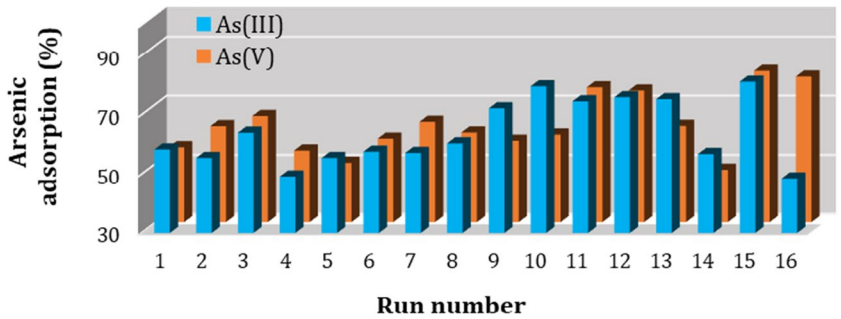

Fig. 6 Percentage removal of **a** As(III) and **b** As(V) vs run number. Experimental condition: [S-nZVI]: 0.05 gm/L; [As] spiked: 5 mg/L; pH: 7.0 ± 0.05

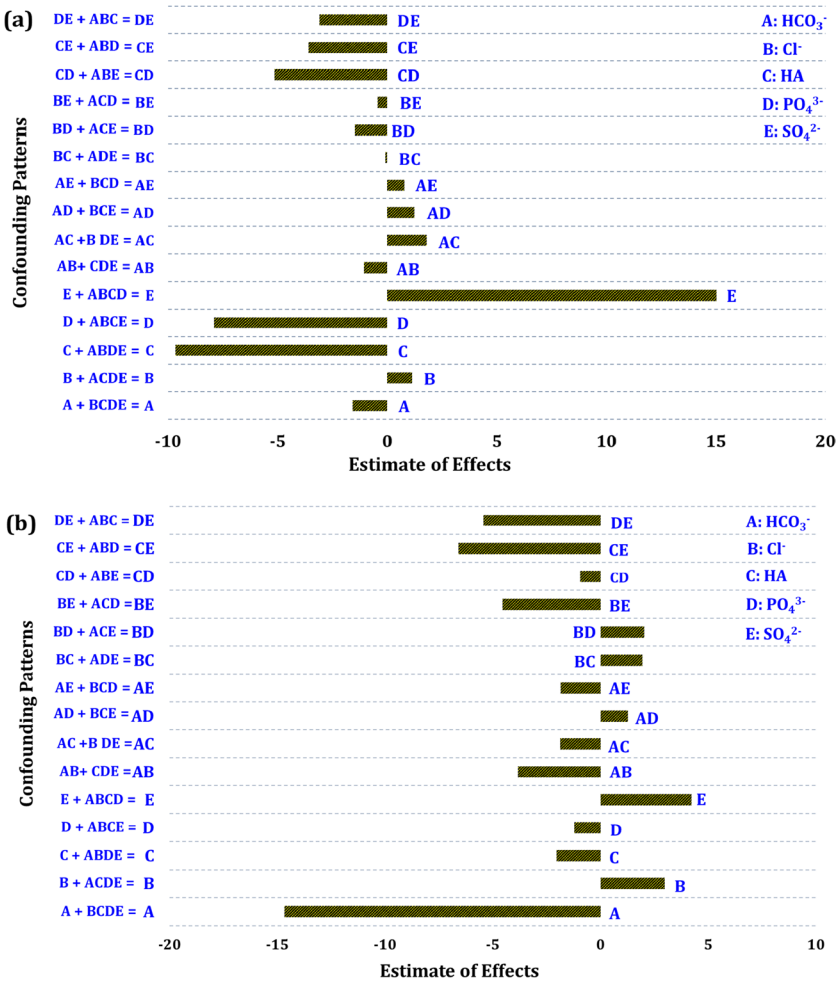

Fig. 7 Estimating the effects of coexisting ions on **a** As(III) and **b** As(V) removal by S-nZVI. Experimental condition: [S-nZVI]: 0.05 gm/L; [As] spiked: 5 mg/L; pH: 7.0 ± 0.05

HA and SO_4^{2-} were the significant main factors for As(III) removal and are in agreement with the results of estimate of effect (Fig. 7a). However, for As(V), the analysis shows that HCO_3^- was the only significant factors and the contribution of other factors such as SO_4^{2-}, Cl^-, PO_4^{3-} and HA was insignificant. This might be expected considering the magnitude of estimate of effects of HCO_3^- for As(V) removal might have surpassed the effect of SO_4^{2-}, Cl^-, PO_4^{3-} and HA ions (Fig. 7b).

Screening of interactive effects

In practical scenario, the coexisting ions investigated may simultaneously affect the arsenic adsorption processes, and thus, the mutual interactive effect needs to be assessed. It should be noted that the combined interaction effect of two factors is not equal to the sum of their individual contributions, but it indicates whether the two factors are antagonistic or synergistic (Tanboonchuy et al. 2012; Liu et al. 2016). For example, as discussed earlier, PO_4^{3-}, SO_4^{2-} and HA of single-factor interaction were most significant for removal of As(III) by S-nZVI. However, the estimate of effect of interaction CD ($HA \times PO_4^{3-}$) was only − 5.15 (Fig. 7a). This value does not only result from ($HA \times PO_4^{3-}$) interaction but was confounded with ($SO_4^{2-} \times Cl^- \times HCO_3^-$). The association can be described as ($HA \times PO_4^{3-}$) = ($HA \times PO_4^{3-}$) + ($SO_4^{2-} \times Cl^- \times HCO_3^-$). Similarly, in the case of As(V) removal by S-nZVI, HCO_3^- was found to be the most dominant factors in one-factor influence analysis, along with HA which had a small negative impact. However, the ($HCO_3^- \times HA$) interaction was not so significant as ($HCO_3^- \times HA$) confounded with ($Cl^- \times PO_4^{3-} \times SO_4^{2-}$); the relationship can be represented as ($HCO_3^- \times HA$) = ($HCO_3^- \times HA$) + ($Cl^- \times PO_4^{3-} \times SO_4^{2-}$) (Fig. 7b).

Figure 8 shows the interaction plot of two factors, with respect to percentage of arsenic removal. Interaction plot is a convenient graphical plot that depicts the mean response of two factors in all conceivable configurations (Antony 2003; Liu et al. 2016). Parallel lines indicate no interaction between the factors; on the other hand, when the lines are non-parallel, there is significant interaction between the two factors (Antony 2003). Furthermore, inside each cell, when the lines have a considerable slope, the interaction due to

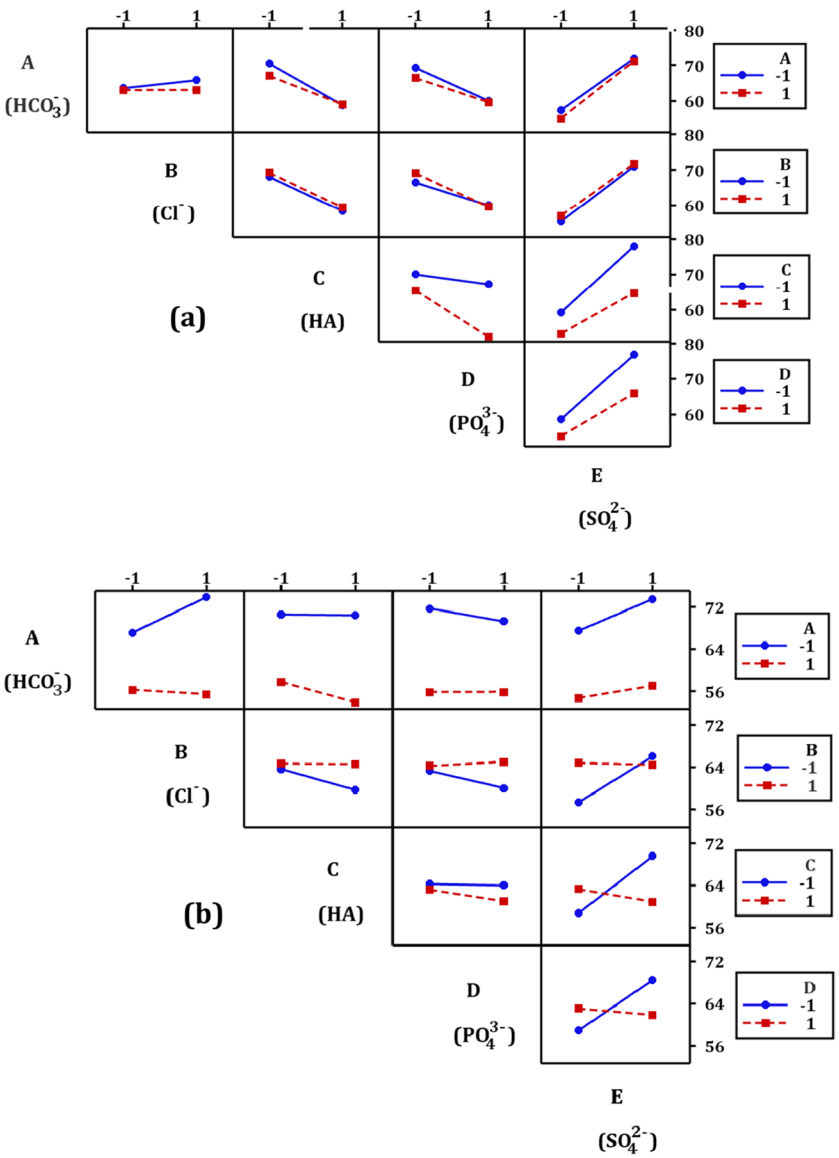

Fig. 8 Interaction effect plot of **a** As(III) and **b** As(V) removal percentage

factor in the *x*-axis is substantial; and the interactions due to factor in the *y*-axis are significant when the separation between the two data points (blue and red) is fairly large (Antony 2003; Tanboonchuy et al. 2012). As for example, in cell AE of Fig. 8a, both the blue and red lines have a positive upward slope, suggesting increase in As(III) removal with increase in factor E (i.e. SO_4^{2-}). On the other hand, the separation between the blue and red points are small, both at high and at low levels of factor A. This indicates insignificant impact of factor A (i.e. HCO_3^-) at both high and low levels on As(III) removal. Moreover, no separate interaction effect exists between SO_4^{2-} and HCO_3^- for As(III) removal as their effect lines are parallel to each other.

Considering the interaction effect between various coexisting ions in the case of As(III) removal, as seen from Fig. 8a, there is significant separation between the blue and red points in row C (HA), D (PO_4^{3-}) and E (SO_4^{2-}), indicating strong impact of these factors on As(III) removal. Therefore, the cells where significant interactions exist is in cell CD, CE and DE. These findings are in concordance with the results in Fig. 7a. The inhibitory role of HA and PO_4^{3-} in As(III) removal is expected and aligns with the published reports on As(III) removal by Fe-based adsorbent (Su and Puls 2001; Bhowmick et al. 2014; Fakour et al. 2015). However, the enhancing effect of SO_4^{2-} on As(III) removal in the presence of other anions is important, highlighting the critical role of surface precipitation of As_2S_3-like phase during the removal of As(III) by S-nZVI (Singh et al. 2021; Zhao et al. 2021). Apart from the above-mentioned cells, small overlapping data points are observed in AC, AD and BD (Fig. 8a). On the other hand, for As(V), significant separation between the blue and red points observed in row A (HCO_3^-) points towards the dominant role of HCO_3^- in As(V) removal (Fig. 8b). This observation corroborates

the findings in Fig. 7b, where similar predominant role of HCO_3^- was identified among the simultaneous presence of all the coexisting ions during As(V) removal. Along with row A, important interactions were also observed in cell BC (high C), BD (high D) and CD (high D) and overlapping interaction was observed in BE, CE and DE. It is interesting to note that for column E (SO_4^{2-}), at lower concentration of HCO_3^-, Cl^-, HA and PO_4^{3-}, there is an increase in As(V) adsorption with increase in SO_4^{2-} concentration (Fig. 8b). Therefore, the present findings suggest that the collective influence of background species on arsenic removal by S-nZVI, when they coexist, may not be a combination of their individual effects, but rather a more intricate relationship may exist.

Conclusion

The present study investigates the mechanism of the influence of co-occurring background ions such as Cl^-, HA, HCO_3^-, PO_4^{3-} and SO_4^{2-} on As(III) and As(V) uptake capacity by S-nZVI. The ions were selected considering their ubiquitous presence in groundwater and their intricate associations with arsenic mobilization processes. Assessment of the individual effect of the background ions showed that both the type and concentration of the ions impacted differently the As(III) and As(V) removal by S-nZVI. Specifically, HA, PO_4^{3-} and SO_4^{2-} had dominant effect on As(III) removal, with HA and PO_4^{3-} hindering the As(III) removal, while SO_4^{2-} facilitated the uptake process. On the other hand, in the case of As(V), HCO_3^- reduced the As(V) uptake capacity by S-nZVI. X-ray investigation of the arsenic-reacted S-nZVI indicates that the background ions modulated the arsenic removal capacity by either competing for the adsorption sites, altering the rate of S-nZVI corrosion reaction or forming different corrosion products. Importantly, the interaction effects demonstrated that when the background ion coexisted together, their cumulative impact on arsenic removal might significantly differ from that in a single-ion system. Overall, this study emphasizes the pivotal role of co-occurring background ions in determining the selectivity of S-nZVI for water treatment, emphasizing their relevance for practical applications of S-nZVI in arsenic abatement. Nonetheless, further research is warranted to elucidate the long-term effects of these coexisting ions on the application of S-nZVI, ensuring its efficacy and sustainability in water treatment processes.

Supplementary Information The online version contains supplementary material available at https://doi.org/10.1007/s11356-024-34596-w.

Author contribution Payel Singh: formal analysis, investigation, data curation, writing—original draft; Penumaka Nagababu: supervision, data curation, writing—review and editing; Manash R. Das: formal analysis, data curation; writing—review and editing; Priyanka Mondal: formal analysis, writing—review and editing; Subhamoy Bhowmick: conceptualization, funding acquisition, methodology, project administration, resources, supervision, writing—review and editing.

Funding Financial support received from Department of Science and Technology, Government of India (DST/INSPIRE/04/2015/002870) is acknowledged. Knowledge Resource Center of CSIR-NEERI is appreciated (KRC No.: CSIR-NEERI/KRC/2022/JAN/KZC-EMD/1).

Data availability The experimental data of this study can be provided by the corresponding author upon reasonable request.

Declarations

Ethics approval Not applicable. This article does not involve studies on human or animal.

Consent to participate Not applicable. This article does not involve studies on human or animal.

Consent for publication All authors have given their consent to publish the manuscript with the journal.

Conflict of interest The authors declare no competing interests.

References

Agrawal A, Tratnyek PG (1995) Reduction of nitro aromatic compounds by zero-valent iron metal. Environ Sci Technol 30:153–160

Antony J (2003) Design of experiments for engineers and scientists. Butterworth-Heinemann, New York

Bhattacharya P, Claesson M, Bundschuh J, Sracek O, Fagerberg J, Jacks G, Martin RA, Storniolo AR, Thir M (2006) Distribution and mobility of arsenic in the Río Dulce alluvial aquifers in Santiago del Estero Province Argentina. Sci Total Environ 358:97–120

Bhowmick S, Nath B, Halder D, Biswas A, Majumder S, Mondal P, Chakraborty S, Nriagu J, Bhattacharya P, Iglesias M, Roman-Ross G, Guha Mazumder DN, Bundschuh J, Chatterjee D (2013) Arsenic mobilization in the aquifers of three physiographic settings of West Bengal, India: understanding geogenic and anthropogenic influences. J Hazard Mater 262:915–923

Bhowmick S, Chakraborty S, Mondal P, Van Renterghem W, Van den Berghe S, Roman-Ross G, Chatterjee D, Iglesias M (2014) Montmorillonite-supported nanoscale zero-valent iron for removal of arsenic from aqueous solution: kinetics and mechanism. Chem Eng J 243:14–23

Bi E, Bowen I, Devlin JF (2009) Effect of mixed anions (HCO_3^- - SO_4^{2-} - ClO_4^-) on granular iron (Fe^0) reactivity. Environ Sci Technol 43:5975–5981

Biswas A, Majumder S, Neidhardt H, Halder D, Bhowmick S, Mukherjee-Goswami A, Kundu A, Saha D, Berner Z, Chatterjee D (2011) Groundwater chemistry and redox processes: depth dependent arsenic release mechanism. Appl Geochem 26:516–525

Box GEP, Hunter JS, Hunter WG (2005) Statistics for Experimenters, 2nd edn. John Wiley & Sons Inc, New York

Bundschuh J, Farias B, Martin R, Storniolo A, Bhattacharya P, Cortes J (2004) Groundwater arsenic in the Chaco-Pampean Plain, Argentina: case study from Robles County, Santiago del Estero Province. Appl Geochem 19:231–243

Deng J, Chen T, Arbid Y, Pasturel M, Bae S, Hanna K (2023) Aging and reactivity assessment of nanoscale zerovalent iron in groundwater systems. Water Res 229:119472

Di L, Chen X, Lu J, Zhou Y, Zhou Y (2023) Removal of heavy metals in water using nano zero-valent iron composites: a review. J Water Process Eng 53:103913

Dong H, Zhang C, Deng J, Jiang Z, Zhang L, Cheng Y, Hou K, Tang L, Zeng G (2018) Factors influencing degradation of trichloroethylene by sulfide-modified nanoscale zero-valent iron in aqueous solution. Water Res 135:1–10

Du Q, Li G, Zhang S, Song J, Zhao Y, Yang F (2020) High-dispersion zero-valent iron particles stabilized by artificial humic acid for lead ion removal. J Hazard Mater 383:121170

Epolito WJ, Yang H, Bottomley LA, Pavlostathis SG (2008) Kinetics of zero-valent iron reductive transformation of the anthraquinone dye Reactive Blue 4. J Hazard Mater 160:594–600

Fakour H, Pan Y-F, Lin TF (2015) Effect of humic acid on arsenic adsorption and pore blockage on iron-based adsorbent. Water Air Soil Pollut 226:14

Filip J, Karlický F, Marušák Z, Lazar P, Černík M, Otyepka M, Zbořil R (2014) Anaerobic reaction of nanoscale zerovalent iron with water: mechanism and kinetics. J Phys Chem C 118:13817–13825

Frau F, Addari D, Atzei D, Biddau R, Cidu R, Rossi A (2010) Influence of major anions on As(V) adsorption by synthetic 2-line ferrihydrite. Kinetic Investigation and XPS Study of the Competitive Effect of Bicarbonate. Water Air Soil Pollut 205:25–41

Garcia AN, Zhang Y, Ghoshal S, He F, O'Carroll DM (2021) Recent advances in sulfidated zerovalent iron for contaminant transformation. Environ Sci Technol 55:8464–8483

Gong Y, Gai L, Tang J, Fu J, Wang Q, Zeng EY (2017) Reduction of Cr(VI) in simulated groundwater by FeS-coated iron magnetic nanoparticles. Sci Total Environ 595:743–751

Gu Y, Gong L, Qi J, Cai S, Tu W, He F (2019) Sulfidation mitigates the passivation of zero valent iron at alkaline pHs: experimental evidences and mechanism. Water Res 159:233–241

Guan XH, Sun YK, Qin HJ, Li JX, Lo IMC, He D, Dong HR (2015) The limitations of applying zero-valent iron technology in contaminants sequestration and the corresponding countermeasures: the development in zero-valent iron technology in the last two decades (1994–2014). Water Res 75:224–248

Han YS, Park JH, Min Y, Lim DH (2020) Competitive adsorption between phosphate and arsenic in soil containing iron sulfide: XAS experiment and DFT calculation approaches. Chem Eng J 397:125426

International Agency for Research on Cancer (IARC) (2012) Arsenic, metals, fibres, and dusts. Volume 100 C. A review of human carcinogens. IARCMonographs on the Evaluation of Carcinogenic Risks to Humans. International Agency for Research on Cancer, World Health Organization, Lyon (France).

Khan KM, Chakraborty R, Bundschuh J, Bhattacharya P, Parvez F (2020) Health effects of arsenic exposure in Latin America: an overview of the past eight years of research. Sci Total Environ 710:136071

Kim E-J, Kim J-H, Azad A-M, Chang Y-S (2011) Facile synthesis and characterization of Fe/FeS nanoparticles for environmental applications. ACS Appl Mater Interfaces 3:1457–1462

Li S, Wang W, Liang F, Zhang W-x (2017) Heavy metal removal using nanoscale zero-valent iron (nZVI): theory and application. J Hazard Mater 322:163–171

Li H, Zhang J, Gu K, Li J (2021a) Sulfidation of zerovalent iron for improving the selectivity toward Cr(VI) in oxic water: involvements of FeS_x. J Hazard Mater 409:124498

Li S, Wu S, Zhang K, Zeng T, Rong L, Wang G (2021b) Fractional factorial design in modeling of polyethyleneimine modified magnetic yeast composites for the removal of uranium with various background ions. J Radioanal Nucl Chem 329:815–827

Liang L, Li X, Lin Z, Tian C, Guo Y (2019) The removal of Cd by sulfidated nanoscale zero-valent iron: the structural, chemical bonding evolution and the reaction kinetics. Chem Eng J 382:122933

Liang L, Li X, Guo Y, Lin Z, Su X, Liu B (2021) The removal of heavy metal cations by sulfidated nanoscale zero-valent iron (S-nZVI): the reaction mechanisms and the role of sulfur. J Hazard Mater 404:124057

Ling L, Zhang W-x (2017) Visualizing arsenate reactions and encapsulation in a single zero-valent iron nanoparticle. Environ Sci Technol 51:2288–2294

Liu C-W, Lai C-C, Chen Y-Y, Lu K-L (2013) Hydrogeochemical and mineralogical investigations of arsenic- and humic substance-enriched aquifers. J Hydrol 498:59–75

Liu S, Wang H, Chai L, Li M (2016) Effects of single- and multi-organic acid ligands on adsorption of copper by Fe_3O_4/graphene oxide-supported DCTA. J Colloid Interface Sci 478:288–295

Liu A, Liu J, Han J, Zhang W-x (2017) Evolution of nanoscale zero-valent iron (nZVI) in water: microscopic and spectroscopic evidence on the formation of nano- and micro-structured iron oxides. J Hazard Mater 322:129–135

Liu X, Cao Z, Yuan Z, Zhang J, Guo X, Yang Y, He F, Zhao Y, Xu J (2018) Insight into the kinetics and mechanism of removal of aqueous chlorinated nitroaromatic antibiotic chloramphenicol by nanoscale zero-valent iron. Chem Eng J 334:508–518

Lv D, Zhou J, Cao Z, Xu J, Liu Y, Li Y, Yang K, Lou Z, Lou L, Xu X (2019) Mechanism and influence factors of chromium(VI) removal by sulfide-modified nanoscale zerovalent iron. Chemosphere 224:306–315

Mak MSH, Rao P, Lo IMC (2009) Effects of hardness and alkalinity on the removal of arsenic(V) from humic acid-deficient and humic acid-rich groundwater by zero-valent iron. Water Res 43:4296–4304

Malik A, Parvaiz A, Mushtaq N, Hussain I, Javed T, Rehman H, Farooqi A (2020) Characterization and role of derived dissolved organic matter on arsenic mobilization in alluvial aquifers of Punjab. Pakistan Chemosphere 251:126374

Mangayayam MC, Alonso-de-Linaje V, Dideriksen K, Tobler DJ (2020) Effects of common groundwater ions on the transformation and reactivity of sulfidized nanoscale zerovalent iron. Chemosphere 249:126137

Matheson LJ, Tratnyek PG (1994) Reductive dehalogenation of chlorinated methanes by iron metal. Environ Sci Technol 28:2045–2053

Mondal PK, Furbacher PD, Cui Z, Krol MM, Sleep BE (2018) Transport of polymer stabilized nano-scale zero-valent iron in porous media. J Contam Hydrol 212:65–77

Montgomery DC (2001) Design and analysis of experiments, 5th edn. John Wiley & Sons Inc, New York

Mu Y, Jia F, Ai Z, Zhang L (2017) Iron oxide shell mediated environmental remediation properties of nano zero-valent iron. Environ Sci Nano 4:27–45

Mundra S, Tits J, Weiland E, Angst UM (2023) Aerobic and anaerobic oxidation of ferrous ions in near-neutral solutions. Chemosphere 335:138955

Nath B, Stüben D, Mallik SB, Chatterjee D, Charlet L (2008) Mobility of arsenic in West Bengal aquifers conducting low and high groundwater arsenic. Part I: Comparative hydrochemical and hydrogeological characteristics. Appl Geochem 23:977–995

Niazi NK, Burton EW (2016) Arsenic sorption to nanoparticulate mackinawite (FeS): an examination of phosphate competition. Environ Pollut 218:111–117

Noubactep C, Kurth A-MF, Sauter M (2009) Evaluation of the effects of shaking intensity on the process of methylene blue discoloration by metallic iron. J Hazard Mater 169:1005–1011

O'Carroll D, Sleep B, Krol M, Boparai H, Kocur C (2013) Nanoscale zero valent iron and bimetallic particles for contaminated site remediation. Adv Water Resour 51:104–122

Palma-Lara I, Martínez-Castillo M, Quintana-Pérez JC, Arellano-Mendoza MG, Tamay-Cach F, Valenzuela-Limón OL, García-Montalvo EA, Hernández-Zavala A (2020) Arsenic exposure: a public health problem leading to several cancers. Regul Toxicol Pharmacol 110:104539

Pincus LN, Rudel HE, Petrović PV, Gupta S, Westerhoff P, Muhich CL, Zimmerman JB (2020) Exploring the mechanisms of selectivity for environmentally significant oxo-anion removal during water treatment: a review of common competing oxo-anions and tools for quantifying selective adsorption. Environ Sci Technol 54:9769–9790

Podgorski J, Berg M (2020) Global threat of arsenic in groundwater. Science 368:845–850

Polasek P (2007) Differentiation between different kinds of mixing in water purification – back to basics. Water SA 33:249–252

Rajajayavel SRC, Ghoshal S (2015) Enhanced reductive dechlorination of trichloroethylene by sulfidated nanoscale zerovalent iron. Water Res 78:144–153

Rangsivek R, Jekel MR (2005) Removal of dissolved metals by zero – valent iron (ZVI): kinetics, equilibria, processes and implications for stormwater runoff treatment. Water Res 39:4153–4163

Shakya AK, Ghosh PK (2018) Simultaneous removal of arsenic, iron and nitrate in an attached growth bioreactor to meet drinking water standards: Importance of sulfate and empty bed contact time. J Clean Prod 186:1011–1020

Shakya AK, Paul S, Ghosh PK (2019) Bio-attenuation of arsenic and iron coupled with nitrate remediation in multi-oxyanionic system: Batch and column studies. J Hazard Mater 375:182–190

Sharma VK, Sohn M (2009) Aquatic arsenic: toxicity, speciation, transformations, and remediation. Environ Int 35:743–759

Singh P, Pal P, Mondal P, Saravanan G, Nagababu P, Majumdar S, Labhsetwar N, Bhowmick S (2021) Kinetics and mechanism of arsenic removal using sulfide-modified nanoscale zerovalent iron. Chem Eng J 412:128667

Su C, Puls RW (2001) Arsenate and arsenite removal by zerovalent iron: effects of phosphate, silicate, carbonate, borate, sulfate, chromate, molybdate, and nitrate, relative to chloride. Environ Sci Technol 35:4562–4568

Sun H, Wang L, Zhang R, Sui J, Xu G (2006) Treatment of groundwater polluted by arsenic compounds by zero valent iron. J Hazard Mater B129:297–303

Sun Y, Li J, Huang T, Guan X (2016) The influences of iron characteristics, operating conditions and solution chemistry on contaminants removal by zero-valent iron: a review. Water Res 100:277–295

Tanboonchuy V, Grisdanurak N, Liao CH (2012) Background species effect on aqueous arsenic removal by nano zero-valent iron using fractional factorial design. J Hazard Mater 205–206:40–46

Turcio-Ortega D, Fan D, Tratnyek PG, Kim EJ, Chang YS (2012) Reactivity of Fe/FeS nanoparticles: electrolyte composition effect on corrosion electrochemistry. Environ Sci Technol 46:12484–12492

Wang S, Gao B, Li Y, Creamer AE, He F (2017) Adsorptive removal of arsenate from aqueous solutions by biochar supported zero-valent iron nanocomposite: batch and continuous flow tests. J Hazard Mater 322:172–181

Wang R, Tang T, Lu G, Zheng Z, Huang K, Li H, Tao X, Yin H, Shi Z, Lin Z, Wu F, Dang Z (2019) Mechanisms and pathways of debromination of polybrominated diphenyl ethers (PBDEs) in various nano-zerovalent iron-based bimetallic systems. Sci Total Environ 661:18–26

Wang L, Wei S, Jiang Z (2020) Effects of humic acid on enhanced removal of lead ions by polystyrene-supported nano-Fe (0) nanocomposite. Sci Rep 10:19663

Watson MA, Tubić A, Agbaba J, Nikić J, Maletić S, Jazić JM, Dalmacija B (2016) Response surface methodology investigation into the interactions between arsenic and humic acid in water during the coagulation process. J Hazard Mater 312:150–158

Wu C, Tu J, Liu W, Zhang J, Chu S, Lu G, Lin Z, Danga Z (2017) The double influence mechanism of pH on arsenic removal by nano zero valent iron: electrostatic interactions and the corrosion of Fe^0. Environ Sci Nano 4:1544–1552

Xu J, Cao Z, Zhou H, Lou Z, Wang Y, Xu X, Lowry GV (2019) Sulfur dose and sulfidation time affect reactivity and selectivity of post-sulfidized nanoscale zerovalent iron. Environ Sci Technol 53:13344–13352

Xu J, Li H, Lowry GV (2021) Sulfidized nanoscale zero-valent iron: tuning the properties of this complex material for efficient groundwater remediation. Acc Mater Res 2:420–431

Yan W, Herzing AA, Kiely CJ, Zhang W-X (2010) Nanoscale zero-valent iron (nZVI): aspects of the core-shell structure and reactions with inorganic species in water. J Contam Hydrol 118:96–104

Yan W, Ramos MAV, Koel BE, Zhang W-X (2012) As(III) sequestration by iron nanoparticles: study of solid-phase redox transformations with X-ray photoelectron spectroscopy. J Phys Chem C 116(9):5303–5311

Yang G, Liu Y, Song S (2015) Competitive adsorption of As(V) with co-existing ions on porous hematite in aqueous solutions. J Environ Chem Eng 3:1497–1503

Yao Y, Mi N, He C, He H, Zhang Y, Zhang Y, Yin L, Li J, Yang S, Li S, Ni L (2020) Humic acid modified nano-ferrous sulfide enhances the removal efficiency of Cr(VI). Sep Purif Technol 240:116623

Zhao X, Liu W, Cai Z, Han B, Qian T, Zhao D (2016) An overview of preparation and applications of stabilized zero-valent iron nanoparticles for soil and groundwater remediation. Water Res 100:245–266

Zhao J, Su A, Tian P, Tang X, Collins RN, He F (2021) Arsenic (III) removal by mechanochemically sulfidated microscale zero valent iron under anoxic and oxic conditions. Water Res 198:117132

Zou Y, Wang X, Khan A, Wang P, Liu YH, Alsaedi A, Hayat T, Wang X (2016) Environmental remediation and application of nanoscale zero-valent iron and its composites for the removal of heavy metal ions: a review. Environ Sci Technol 50:7290–7304

Zubair YO, Fuchida S, Tokoro C (2022) Adsorption and microscopic analysis of arsenate uptake by magnetic Fe nanoparticles: a detailed study on coexisting anions effects. Water Air Soil Pollut 233:484